

2005 Volcano-Tectonic Earthquakes Swarm in the Andaman Sea: Triggered by the 2004 Great Sumatra-Andaman Earthquake

Bhaskar Kundu^{1*}, Denis Legrand², Kalpna Gahalaut¹, Vineet K Gahalaut¹, P. Mahesh¹, K.A. Kamesh Raju³, J.K. Catherine¹, A. Ambikapthy¹, R.K.Chadha¹

1. National Geophysical Research Institute (CSIR), Hyderabad-500007, India
2. UNAM, Instituto de Geofísica, Av. Universidad 3000, Ciudad Universitaria, Del. Coyoacán, C.P. 04510. México D.F. México.
3. National Institute of Oceanography (CSIR), Dona Paula, Goa-403004, India

*Corresponding Author (Email: rilbhaskar@gmail.com)

Abstract:

A 6-days duration earthquakes swarm occurred in the Andaman Sea, 31 days after the giant 2004 Sumatra-Andaman earthquake (Mw 9.2). The swarm occurred less than 100 km from the eastern edge of the 2004 earthquake rupture and is the most energetic ever recorded in the world. The earthquakes of the swarm appear to have occurred on en-échelon fault system bounded by the two main right-lateral strike slip faults, namely, the Seulimeum Strand of Sumatra Fault system (SEU) and the West Andaman Fault (WAF). At the beginning of the swarm, earthquakes with predominantly strike-slip focal mechanisms occurred which were followed by earthquakes with predominantly normal faulting focal mechanisms having significant deviatoric component. High b-value, presence of double slope in the Gutenberg-Richter relation, presence of monogenetic submarine volcanoes in the region of the swarm and the earthquake focal mechanisms suggest that the swarm was of volcano-tectonic origin and fluid flow played an important role in its occurrence. Indeed, our modeling suggests that it was triggered by the 2004 Sumatra-Andaman earthquake through poroelastic relaxation of the coseismic stresses.

Keywords: Sumatra-Andaman earthquake, en-échelon, volcano-tectonic earthquakes swarm, b-value.

1. Introduction

“Earthquake sequence” can be considered as a sequent of events (e.g., mainshock³⁴ aftershock sequence, foreshock sequence, aftershock sequence, foreshock-mainshock³⁵ aftershock sequence, earthquake swarm etc.) in space and time with respect to background seismicity of the region (Mogi, 1963). An “earthquake swarm” can be characterized by many events nearly of same size without a distinct mainshock in earthquake sequence (Mogi, 1963). An earthquakes swarm may be of a pure tectonic origin, a pure volcanic origin or a combination of both. Examples of such diverse types of earthquakes swarm were reported globally (e.g., Omori, 1895; Sykes, 1970; Einarsson, 1986, 1991, Brandsdóttir and Einarsson, 1992; Toda et al., 2002; Legrand et al., 2002; Legrand et al., 2011; Wright et al., 2012). However, their origin, mechanism, spatio⁴³ temporal and magnitude distributions of the earthquakes swarm are poorly understood. The prime causes of most of the earthquakes swarm are the stress changes in the shallow and brittle crustal due to fluid flow such as magmatic intrusions, tectonic faulting or hydrothermal cooling which result in an increase in the number of earthquake productivity (Sykes 1970; Nur, 1974). The magnitude distribution of both tectonic and volcanic swarms are described by the Gutenberg-Richter (GR) law, where the b-value (i.e., slope of the log of cumulative frequency versus magnitude distribution) describes the relative proportion of small and large magnitude events (Gutenberg and Richter, 1944). For tectonic swarms, although, b-value is globally close to one (Gutenberg and Richter, 1954, Lay and Wallace, 1995), it can vary both at local and regional scales (Wiemer and Wyss, 1997) depending upon tectonic regime. Relatively higher b-values are related to low stress conditions (Scholz, 1968), higher pore pressure (Wiemer et al., 1998), or greater heterogeneity and variability in the distribution of fractures (Wyss 1973; Wyss and Habermann, 1988, Wyss et al., 2004). In contrast, b-values of volcanic swarms are significantly larger than one ($b=3$) (Francis, 1968a; 1968b; Francis, 1974; Hill et al., 1989; Matsumura et al., 1991; Wiemer and McNutt, 1997). The rate and epicentral distribution of such volcanic swarm events may vary significantly over the course of the dyke intrusion process in the oceanic crust and propagation laterally, subsequently earthquakes are nucleated by breaking around the dike tip and they follow the dike propagation (Hill et al., 1989; Toda et al., 2002). In a recent study of dynamic rifting process, Wright et al., (2012) presented a more realistic picture about seismic activity and its associated rifting episodes from the two subaerial mid-oceanic ridges (i.e., Iceland and Afar region in Africa). It was proposed that the magma moves through complex plumbing systems and multiple magma storage systems seem to interact and feed laterally propagating dykes during rifting episodes (Wright et al., 2012).

Triggered earthquakes and swarms are commonly observed in response to stress changes due to regional and local events as well as due to the passage of seismic waves from large distant earthquakes (Brodsky et al., 2000; Brodsky and Prejean, 2005). In the active back arc rift systems we anticipate dominance of triggered seismic swarms because the fault systems extending into the brittle crust remain very close to the failure. Stress may be amplified in the brittle zones that surround the magma bodies and hot ductile region resulting from submarine volcanism. Thus strong earthquakes may perturb hydrothermal systems by opening a juvenile passage. A number of time dependent processes, including afterslip, pore-fluid flow and viscoelastic relaxation of the lower crust and upper mantle may further modify the pore-pressure induced stresses near the fault, and hence they may influence the seismic swarm. If fluids are present in the upper to middle crust, pore pressure change may be induced by the sudden change in the stress field because of the occurrence of major and great earthquakes and the decay of induced pore pressure obeys diffusion law. Many examples of the generation of aftershocks have been explained by the time-dependent pore pressure effect of the postseismic process (e.g., Bell and Nur, 1978; Rudnicki, 2001; Gahalaut et al., 2008), but very few cases of triggered seismic swarms by the large earthquakes have been studied. One such swarm occurred in the Andaman Sea, the back arc region of Sumatra-Andaman subduction zone, between the Car-Nicobar and Great Nicobar Islands of India (at about 8°N and 94°E) during January 2005, following the Mw 9.2 December 26, 2004 Sumatra-Andaman earthquake (Fig. 1). Here in this article, we use the relocated earthquakes of the swarm (the EHB catalogue of ISC) and analyse them. We discuss the spatiotemporal evolution of the swarm, its characteristics, and possible mechanism involving time-dependent porepressure induced stress modification on the causative faults.

2. Geodynamic setting of the Andaman Sea region

Plate motion between the Indo-Australia and Sunda plates along the Andaman Sumatra convergent plate margin is oblique, with a relative velocity of about 4 cm/year (Fig. 1). As a result of oblique relative motion, slip partitioning occurs, in which predominantly arc normal motion occurs in the fore arc while in the back arc predominantly arc parallel motion occurs. The region between the fore arc and back arc is referred as the Burma sliver plate. The arc parallel motion in the back arc is accommodated through dextral strike slip motion along the approximately north-south oriented Sumatra Fault System (SFS), West Andaman Fault (WAF), Seulimeum Strand of SFS (SEU), and Eastern Margin Fault (EMF) etc. and normal and strike-slip faulting in the Andaman sea-ridge transform fault system where Andaman Sea opening takes place. The geodynamic framework of the Andaman Sea region is very complex. It has been described as a pull-apart basin rather than a typical extensional back-arc basin (Curry et al., 1982; Curry, 1989; Raju et al., 2004; Curry, 2005).

Physiographic features of the Andaman Sea includes the Alcock and Sewell rises, central Andaman basin between the two submarine rises, and numerous smaller topographic features like monogenetic volcanoes and other features of unknown origin. The principal spreading occurs in between the Alcock and the Sewell submarine rises along the Andaman Spreading Ridge (ASR) and as a consequence, several transform faults develop between segments of spreading ridges, well up to the northern tip of the Sumatra Island (Curry, 2005) (Fig.2).

3. Earthquake swarm history of the Andaman Sea

The back arc basin in the Andaman Sea region has experienced three distinct phases of swarm activities in past five decades, namely, during 1983-1984, 1993 and 2005 (Fig.1). The 1983-1984 swarm (16 December 1983 to 13 August 1984) consisted of about 180 seismic events ($3.5 < M_w < 5.5$). During the period of December 1983 to March 1984, the swarm clustered along the eastern side of the Alcock Rise (at around 13°N and 95.5°E) on the NE-SW oriented ASR. During the period from April to August 1984, the swarm migrated to about 230 km further south and clustered along the central spreading ridge segment between Alcock and Sewell ridges (at around 11°N and 95°E) (Fig.1). The 1993 swarm (23 August to 29 October 1993) included only about 35 seismic events ($3.5 < M_w < 5$) that were clustered at the southwest segment of the central ASR (at about 10°N and 94.2°E) (Fig.1). It may be noted that this swarm in ASR coincided with one of the volcanic episode at the Barren Island (March 1991 to May 1995) and most interestingly, this swarm initiated exactly at the same place where the previous 1984 swarm ceased and further proceeded towards southwest to terminate along the WAF. Unlike previous two phases of swarm activities, the 2005 swarm is the most energetic ever observed globally (Lay et al., 2005) which followed the great Sumatra Andaman earthquake of 26 December 2004. We discuss this swarm in great detail in the subsequent sections.

4. Characteristics of the 2005 Andaman Sea earthquake swarm

Following salient characteristic features are documented for the 2005 swarm:

- The swarm occurred during very short period of time (26-31 January, 2005) and a total of about 650 events of $3.9 < M_w < 5.9$ from relocated earthquake catalogue (EHB catalogue) are recorded (Fig.3). The swarm occurred mainly in a single phase in the Andaman Sea back-arc basin involving more than 150 events of $M > 5$ and the major pulse was recorded on 27-28 January (>200 events/day of $M_w > 5$).
- The epicentral location of the earthquakes of the swarm show an elongated NE SW trending zone with a strike wise length of about 90 km and a width at about 60 km across the WAF and SEU

(Fig.2). Here we have used the epicentral locations as given in the EHB catalogue and have not tried to improve them due to non-availability of near source seismic stations. Typical error in these locations is less than 10 km (Engdahl et al., 1998) which does not affect the broad conclusions of such an exercise.

- Interestingly, unlike the epicentral clusters of 1983-1984 and 1993 swarms, the 2005 swarm is located (at about 8°N and 94°E) in the region between the WAF and SEU which has not been previously identified as spreading rift segment. Curray (2005) identified it as a possibly inactive spreading axis.
- Motion during the earthquakes at the beginning of the swarm was predominantly of strike-slip type. The first earthquake with a predominant normal faulting mechanism appeared only after a day of the initiation of the swarm. After that, the mixed episodes of earthquakes with predominant normal and predominant strike slip are noticed (Figs.3 and 4).
- Presenting detailed seamount morphology, swath bathymetric data (Fig.5), analysis of the seabed samples (i.e., particularly ferromanganese oxides from the crater-floor and the flank), Raju et al. (2012) suggested the presence of two submarine volcanoes in the region of 2005 earthquakes swarm. Further, no unusual degassing was reported during swarm activity (Walter and Amlung, 2007).

5. Temporal variation in the sense of motion during the swarm

The initiation of the seismic swarm on January 26, 2005 and its evolution in the next 5 days is quite interesting. Although, the epicentral locations do not show any temporal variation, like swarm associated with laterally propagating magmatic dyke intrusion in a typical spreading ridge segments (Einarsson and Brandsdóttir, 1980, Einarsson, 1991, Wright et al., 2012), there is a significant temporal variation in the mode of faulting as seen in the earthquake focal mechanism solutions. Earthquakes in the beginning of this swarm were characterized with predominant strike-slip motion, but in later period the earthquakes involved both normal and strike-slip motion (Fig.3 and 6) on NE-SW oriented planes. We propose that the swarm was actually initiated on the WAF through dextral strike-slip motion on the NNW-SSE oriented fault but then in the later period, the right step over region of the 'en échelon' fault system, forming a releasing bend, got activated to produce predominantly normal faulting earthquakes.

We analyzed the stress state in the region and its temporal evolution through the inversion of the earthquake focal mechanisms. We used the linear least square inversion approach (Michael, 1984,

1987) to estimate the best fitting maximum (s_1), intermediate (s_2) and minimum (s_3) stress directions. We find that prior to the 2004 Sumatra-Andaman earthquake, the stress system was conducive for predominant thrust faulting in the frontal arc and dextral strike-slip faulting on the WAF in the back arc. The direction of maximum principal stress was in the NNE-SSW with almost zero plunge. The stress system derived from the earthquakes of the first 24 hours of the swarm was identical to that of the pre-2004 stress state. However, the stress state in the following 5 days (i.e., 27th-31st January, 2005) is slightly different, in which the direction of maximum principal stress did not change much but its plunge changed significantly from 0° to 27° (Fig.6). We argue here that such change is significant and is more than the uncertainties (McCaffrey, 1992) involved in such parameters of an earthquake's focal mechanism. This stress state is significantly different from that during the first day or the pre-2004 period, and it caused major change in the sense of motion during the earthquakes. In such a stress state, both types of faulting (dextral strike-slip faulting on the NW-SE oriented fault and normal faulting on the NE-SW oriented fault) are consistent with a single stress state. This is because s_1 which is optimally oriented for dextral strike-slip faulting on NW-SE oriented faults became almost parallel to the NE-SW oriented fault planes with normal motion and its effect was neutralized in the normal faulting, and hence the sub vertical s_2 and horizontal s_3 promoted normal motion on the NE-SW oriented planes. Further, we analyzed the static .CFS on the favorably oriented normal faults (with NE SW oriented planes) due to the dextral strike-slip on the NW-SE oriented fault under the above regional stress system and found that the strike-slip faulting indeed facilitated normal faulting supporting the previous observation of temporal change in the focal mechanisms.

6. b-value of the 2005 Andaman Sea swarm

We analyzed the GR relation for the seismicity of the Sumatra-Andaman region during the period from 1973 to 2010. The b-value of the GR law was calculated with the maximum likelihood method (Aki, 1965) in case of a single slope (Fig.7, curve 'C'). However, in the case of a double slope (Fig.7, curve 'A' and 'B') we used the method of Shimazaki (1986). For the earthquakes of entire region (15° longitude/ 15° latitude spatial window) that includes the 2005 Andaman Sea swarm, but excludes the swarms that occurred during year of 1983-1984 and 1993 in the ASR (Fig.7, curve 'A'), we found that the magnitude and earthquake frequency relation can be better represented by two different b values, viz., $b_1=1.02\pm 0.03$ for lower magnitude earthquakes and $b_2=1.45\pm 0.07$ for higher magnitude earthquakes. The break in the slope at magnitude 5.2-5.3 is quite apparent. Then we calculated the b value for the 2005 Andaman Sea swarm alone (Fig.7, curve 'B'). The double slope with two different b values, viz., $b_1=1.1\pm 0.03$ and $b_2=1.66\pm 0.28$ and the break in slope were still

present. Finally, the GR law was analyzed for the entire region, but excluding the 2005 Andaman Sea swarm and also the swarms that occurred during year of 1983-1984 and 1993 in the ASR (Fig.7, curve 'C'). In this case, only a single slope is observed, with a b value as 1.02 ± 0.03 . Thus it appears that the break in the slope is real and not the result of an incomplete catalogue or some artifact of the analysis.

7. 2005 swarm as a result of poroelastic stress change caused by the 2004 Sumatra Andaman earthquake

We suggest that the poroelastic relaxation of the coseismic stresses due to the 2004 Sumatra-Andaman earthquake significantly influenced the occurrence of the swarm and its location. In fact, high b value and break in slope in the GR relation is possibly an indicator of role of fluid in the occurrence of the swarm. All along the Andaman Sumatra region, the back arc in the Nicobar region, where the 2005 swarm is centered, is at the closest distance from the surface projected 2004 Sumatra Andaman earthquake rupture (Gahalaut et al., 2006, Gahalaut et al., 2008, Banerjee et al., 2007, etc.) in the frontal arc. Interestingly, it is in this part of the rupture where coseismic slip was the maximum. The shorter distance between the rupture and the swarm region and the higher slip on the earthquake rupture in this region imply greater stress transfer from the 2004 earthquake source region to the region where 2005 swarm occurred. But the fact that the swarm did not initiate immediately after the earthquake but after 31 days, suggests redistribution of stresses, possibly through poroelastic relaxation. We explore this possibility in this section. The viscoelastic relaxation mechanism typically operates over a period of several months to years and hence is not explored here.

Postseismic Coulomb failure stress (.CFS) modification because of poroelastic relaxation may qualitatively explain the spatiotemporal variation in the seismicity (e.g., aftershock, seismic swarms etc). In fact, aftershocks, and earthquake swarms in this case, do not all occur instantaneously following the main event and there is a time delay which depends upon the .CFS modification, magnitude and slip distribution on the rupture, nature of poorly understood diffusion process and also spatial distribution of the critically stressed fault zones in the surrounding region. Pore pressure gradients produced by the coseismic stress in the surrounding rock mass eventually dissipate as crustal fluids mobilize in the days, weeks and months after the main event (Peltzer et al., 1998). Presence of brecciated fault zones further provide suitable channel for subcrustal fluid flow and influence the temporal stress evolution (Mitchell and Faulkner, 2008).

We compute postseismic stress changes due to the poroelastic stress relaxation in the surrounding volume containing the main fault zone. The prime assumption of this modeling is that the stress-strain relation is governed by linear, undrained poroelasticity and the flow of fluids in the porous crust follows the mass diffusion law described by Darcy's law (Wang, 2000). We have used the rupture geometry and slip distribution on the rupture segment of the 2004 Sumatra-Andaman earthquake in our coseismic model (Gahalaut et al., 2006) to compute time-dependent .CFS change on the WAF, in the one month following the 26th December 2004 Sumatra-Andaman earthquake. .CFS is defined as:

$$\Delta\text{CFS} = \Delta\tau - \mu(\Delta\sigma - \Delta p)$$

where μ is the frictional coefficient and the Δ represents changes in normal (σ), shear (τ) and pore pressure (p) since the 2004 Sumatra Andaman earthquake. Diffusion of pore pressure is calculated following the approach of Gahalaut et al., (2008) that used Green's function based stress diffusion solutions in the porous elastic medium. We used undrained Poisson's Ratio as 0.25, hydraulic diffusivity as 1.0 m²/s, Skempton's coefficient as 1, and the friction coefficient as 0.6 (Talwani and Acree, 1984; Talwani et al., 2007; Gahalaut et al., 2008). Positive .CFS encourages failure on the considered fault plane and vice-versa. We find that the instantaneous .CFS due to coseismic slip on the 2004 earthquake rupture is positive in the region of swarm and on the WAF. Hence the occurrence of the 2004 earthquake encouraged failure on the WAF, mainly through decrease in normal stress, i.e., unclamping. At the centre of the swarm, .CFS was about 7 bar (Fig.8). In the subsequent period of one month, the increase in pore pressure further increases the .CFS. 31 days after the 2004 earthquake, .CFS increased from 7 bars to 10 bars in the epicentral region of 2005 swarm due to the relaxation of pore pressure (Fig.9). Thus the increase in stress is mainly because of unclamping effect caused by the 2004 Sumatra Andaman earthquake on the WAF and the increase in pore pressure. We propose that the increase in stress by about 10 bar caused failure on the segment of WAF which was critically stressed for failure, which led to the initiation of the swarm.

8. Discussion

8.1. Sensitivity in the computations related to .CFS

The quantitative values in the computations related to poroelastic relaxation of the Coulomb stress are dependent on rupture geometry of the 2004 Sumatra Andaman earthquake, coseismic slip distribution, elastic properties and hydraulic diffusivity of the medium, and the nature of the fault on which the Coulomb stress is resolved. However, adopting a different rupture model (e.g., Banerjee et

al., 2007; Ammon et al., 2005) for the earthquake, and variation in any of other quantities does not change the results qualitatively in any significant manner. Thus within the slight variation in the rupture models, regional stress direction, rheology and hydrological properties of the medium, the results are stable.

The deformation following the 2004 Sumatra Andaman earthquake has also been modeled using the frictional afterslip (Paul et al., 2007; Gahalaut et al., 2008). The afterslip patch in the Nicobar region partly overlaps with the coseismic rupture of the 2004 Sumatra Andaman earthquake. Thus, the stress change caused by the afterslip patch on the swarm region is similar to that by the coseismic rupture. In both cases the stress change is positive but the magnitude in case of afterslip patch will be less due to lesser slip on the afterslip patch as compared to the higher coseismic slip. Thus, even in the case when we consider postseismic deformation to be governed by the afterslip, the stress change is positive in the region of swarm and thus encourages slip on the earthquake causative faults of the swarm. However, as discussed earlier, in the initial period of postseismic deformation following the 2004 Sumatra-Andaman earthquake, it is the poroelastic relaxation which should dominate.

8.2. Is the swarm associated with active submarine volcanism?

A recent study in the southern Andaman Sea region reported steep-sided twin monogenetic volcano near the center of the earthquake swarm (Raju et al., 2012). The volcanic nature of the cratered mount was deduced from the seamount morphology identified by swath bathymetric data, sample analysis of the seabed, showing ferromanganese oxides of the crater-floor and from the flank (Raju et al., 2012). Recovery of dacites and andesitic rocks from the crater indicates the eruption of re-melted subducting lithosphere, normally found at arc-stratovolcanoes e.g., volcanoes of Andaman-Sumatra arc (Rittmann, 1953), Kermadec-arc, (Wright, 1996), Kurile-arc, (Glassby et al., 2006). This extensive study suggests that the submarine volcanoes have not erupted in recent few decades in the Andaman Basin. In another study, a nascent rift supported by the magmatic dyke injection hypothesis has been speculated (Mukhopadhyaya et al., 2010). However, in view of our analysis and the studies by Raju et al., (2012) we suggest that the swarm has tectono-volcanic origin.

8.3. Significance of double slope in Gutenberg-Richter law in the 2005 Andaman Sea swarm

We interpreted the GR law of the 2005 swarm as a double slope. Hence, it is important to assess whether such double slope is real and is not an artifact due to the incompleteness of the earthquake catalogue. The b-value of the whole region without any swarm during the period 1973-2010 shows a perfect GR law, with a value of 1.02, typical of seismicity of tectonic origin. This

value is close to the typical b value of about 1.0 and may be considered as the regional global average b -value. The magnitude of completeness (M_c) for earthquakes is 4.5 (which corresponds to the magnitude from where onwards the curve of the GR is linear). For the 2005 swarm too, the M_c is 4.5 because this swarm is included within the whole region for which M_c is 4.5. As a consequence, we can calculate the b -value of this swarm using M_c as 4.5. However, we notice that in this case we have two slopes, which are real because of the value of M_c and the following reasons. The b -value between $M_c=4.5$ and $M_{break}=5.2$ is 1.1, which is very close to the whole region (1.02). From $M_{break}=5.2$ and $M_{end}=5.8$, b -value is 1.6. We consider that this value is also real because the swarm only lasted 5 days and that we are sure that the global network of seismographs operated by the USGS, did not miss earthquakes of $M > 5$ in that region during those 5 days. Hence, we definitely have a lack of large events (M_w between 5.0 and 5.8) and not a lack of small events (M_w between 4.5 and 5.0), which is leading to two slopes in the GR law and higher b value for the higher magnitude earthquakes of the swarm. Various explanations have been proposed to explain high b -values: (1) highly heterogeneous materials submitted to mechanical loading (Mogi, 1962) and/or the presence of highly porous rocks, within which the proportion of microfractures is greater than in a less porous rock (Scholz, 1968), (2) since the effective normal stress decreases with higher pore pressure, it may influence microfracture formation, which may further lead to high b values (e.g., in reservoir induced seismicity, Simpson et al., 1988), (3) decrease in the amplitude of the stress field (Scholz, 1968; Wyss, 1973), (4) nature of the rock materials (e.g., ductile rock has a higher b values than a brittle rock) (Scholz, 1968), and (5) high temperatures may also increase b -values (Warren and Latham, 1970).

In the 2005 swarm, the double slope in GR law with two different b -values appears to be real and has significant implication. We suggest that in this case, the break may be due to the presence of fluids (which could be water and/or magma) or due to increase in temperature in that region. As another study in that region has revealed presence of very close two monogenetic volcanoes (Raju et al., 2012), we suggest that this swarm is generated by the movement of magma and the presence of elevated temperatures at 10-30 km depths (corresponding to the depth of the seismicity, see Fig 8). The magma did not reach the surface as evident from the lack of shallow seismicity and evidence of no degassing (Walter and Amelung, 2007). Wright et al., (2012) presented seismic activity associated with subaerial segments of mid-oceanic ridges (i.e., Iceland and Afar region in Africa) and suggested that it can be used to identify the magmatic plumbing system. Such kind of magma migration without reaching to the surface has been reported elsewhere too and is common in spreading environments (e.g Roman et al., 2004; Legrand et al., 2011; Wright et al., 2012).

8.4. Feed-back tectonic and volcanic responses

The 2005 Andaman swarm is related to both tectonic and volcanic processes. The swarm probably occurred on the WAF and on the en-échelon faults joining the WAF and SEU. The swarm initiated on the WAF through dextral strike slip motion. The focal mechanisms of the strongest earthquakes of this swarm on the next four days have significant deviatoric (double couple, DC + compensated linear vector dipole, CLVD) component and many events exhibit normal focal mechanisms. The extension component corresponds to the opening of a basin in a pull-apart fault system where monogenetic volcanoes have been identified. Nevertheless, the focal mechanisms of all the earthquakes are compatible with a unique stress tensor (Fig. 6). Thus the time evolution of the focal mechanism shows the feedback response of the tectonic behavior of this swarm (strike-slip focal mechanisms almost on the right-lateral WAF) and the volcanic behavior (normal focal mechanism within the pull-apart system). This swarm allows us to indirectly locate with a fair precision the existence of an 'en échelon' fault system between the WAF and SEU faults, which is important as these faults are deep-seated and are under water in that part of the subduction zone.

9. Conclusions

Our analysis of the 2005 swarm leads us to the following conclusions:

1. We suggest that the 2005 Andaman Sea earthquakes swarm was triggered by the 2004 great Sumatra-Andaman earthquake (Mw 9.2). Further, we suggest that the delay in triggering is due to the poroelastic response of the medium to the elastic stress change caused by the earthquake.
2. We propose that poroelastic stress modulations triggered strike-slip earthquake on the WAF which in turn promoted earthquakes with normal motion in the region between WAF and SEU.
3. Despite diversity in the focal mechanisms of the earthquakes of the swarm, a single stress system, consistent with the regional tectonics, can be derived from this swarm.
4. This swarm probably has a tectonic as well as volcanic origin, and both are intimately linked to each other in a retro feed-back dynamic manner. The tectonic origin is represented by the strike-slip focal mechanisms, compatible with the reactivation on the WAF. The volcanic origin is represented by the normal faults and the significant deviatoric part in the earthquake focal mechanisms. Further, the double slope (with $b_1=1.1$ and $b_2=1.6$) in the Gutenberg-Richter law of the 2005 Andaman Sea earthquakes swarm is probably due to the superposition of two distinctly different physical processes (i.e., the classical elastic fracture formation for b_1 and fluid induced

hydraulic fracture formation for b2). The presence of monogenetic volcanoes just above the seismicity supports the volcanic context of this swarm.

5. Seamount morphology, seafloor images by swath bathymetric data, analysis of the seabed samples particularly ferromanganese oxides from the crater-floor and the flank, and most importantly, the absence of unusual degassing, suggest that the swarm was not associated with nascent rifting episode or with active submarine volcanic phenomenon.

Acknowledgements

The work is a result of a joint research project between India and Mexico supported by the Department of Science and Technology, New Delhi and CONACYT, Mexico. The manuscript was improved by thoughtful comments of Joseph Curray, Páll Einarsson and two anonymous reviewers. We also benefited from the encouraging comments by the editor, Todd Ehlers and associate editor, Rebecca Bendick.

References:

- Aki, K. (1965), Maximum likelihood estimate of b in the formula $\log N = a - bM$ and its confidence limits, *Bull. Earthquake Res., Inst. Univ. Tokyo*, 43, 237–239.
- Bell, M.L., and Nur, A., (1978), Strength changes due to reservoir-induced pore pressure and stresses and application to Lake Oroville., *J. Geophys. Res.*, 83, 4469–4483.
- Brandsdóttir, B., and P. Einarsson. (1992), Volcanic tremor and low-frequency earthquakes in Iceland. In: *Volcanic Seismology* (eds. P. Gasparini and K. Aki), Springer Verlag, 212–222.
- Brodsky, E. E., and Prejean, S.G., (2005), New constraints on mechanisms of remotely triggered seismicity at Long Valley Caldera, *J. Geophys. Res.*, 110, B04032, doi:04010.01029/02004JB003211.
- Brodsky, E. E., Karakostas, V., and Kanamori, H., (2000), A new observation of dynamically triggered regional seismicity: Earthquakes in Greece following the August, 1999 Izmit, Turkey earthquake, *Geophys. Res. Lett.*, 27, 2741–2744.
- Chlieh, M. et al., (2007), Coseismic slip and afterslip of the great (Mw9.15) Sumatra– Andaman earthquake of 2004, *Bull. seism. Soc. Am.*, 97, S152–S173.
- Curray, J.R., Emmel, F.J., Moore, D.G., and Raitt, R.W., (1982), Structure, tectonics and geological history of the northeastern Indian Ocean. In: Nairn, A.E.M., Stehli, F.G. (Eds.), *The Ocean Basins and Margins., The Indian Ocean*, vol. 6. Plenum Press, New York, pp. 399–450.
- Curray, J.R., (1989), The Sunda Arc: a model for oblique plate convergence, Netherlands, *Journal of Sea Research*, 24, 131–140.
- Curray, J. R., (2005), Tectonics and history of Andaman sea region, *J. Asian Earth Sci.*, 25, 187–232.

- Einarsson, P., and Brandsdóttir, B., (1980), Seismological evidence for lateral magma intrusion during the July 1978 deflation of the Krafla volcano in NE-Iceland, *J. Geophys.*, 47, 160-165.
- Einarsson, P., (1986), Seismicity along the eastern margin of the North American Plate. in Vogt, P.R., and Tucholke, B.E., eds., *The Geology of North America, Vol. M, The Western North Atlantic Region: Geological Society of America*, 99-116.
- Einarsson, P., (1991), Earthquakes and present-day tectonism in Iceland. *Tectonophysics*, 189, 261-279.
- Engdahl E R, Hilst R. V. D. and Buland R., (1998), Global teleseismic earthquake relocation with improved travel time and procedures for depth determination; *Bull. Seismol. Soc Am.* 88, 722–743.
- Francis, T., (1968a), The detailed seismicity of mid-oceanic ridges, *Earth Planet. Sci. Lett.*, 4, 39–46.
- Francis, T. (1968b), Seismicity of mid-oceanic ridges and its relation to properties of the upper mantle and crust, *Nature*, 220, 899–901.
- Francis, T. (1974), A new interpretation of the 1968 Fernandina caldera collapse and its implications for the mid-oceanic ridges, *Geophys. J. R. Astron. Soc.*, 39, 301– 318
- Gahalaut, V.K., Nagrajan, B., Catherine, J.K. and Kumar, S., (2006), Constraints on 2004 Sumatra–Andaman earthquake rupture from GPS measurements in Andaman-Nicobar Islands, *Earth planet. Sci. Lett.*, 242, 365–374, doi:10.10116/j.epsl.2005.11.051.
- Gahalaut, V.K. et al., (2008), GPS measurements of postseismic deformation in the Andaman-Nicobar region following the giant 2004 Sumatra–Andaman earthquake, *J. geophys. Res.*, 113, B08401, doi:10.1029/2007JB005511.
- Gahalaut, K., Gahalaut, V.K. and Kayal, J.R. (2008), Poroelastic relaxation and aftershocks of the 2001 Bhuj earthquake, India, *Tectonophysics*, doi:10.1016/j.tecto.2008.07.004
- Glasby G.P., G.A. Cherkashov, G.M. Gavrilenko, V.A. Rashidov, and I.B. Slovtsov, (2006), Submarine hydrothermal activity and mineralization on the Kurile and western Aleutian island arcs, N.W. Pacific, *Mar. Geol.*, 231,163-180
- Gutenberg, B., and Richter, C.F., (1944), Frequency of earthquakes in California, *Bull. Seismol. Soc. Am.*, 34, 185–188
- Gutenberg, B., and Richter, C., (1954), *Seismicity of the Earth and Associated Phenomena*, 2nd ed., Princeton Univ. Press, Princeton, N. J.
- Hill, D., (1977), A model for earthquake swarms, *J. Geophys. Res.*, 82, 1347–1352.
- Lay, T. et al., (2005), The Great Sumatra–Andaman earthquake of 26 December 2004, *Science*, 308, 1127–1133.
- Lay, T., and Wallace, T., (1995), *Modern Global Seismology*, 521 pp., Academic Press, San Diego, California.

Legrand D., Barrientos S., Bataille K., Cembrano J., and Pavez A., (2011), The fluid driven tectonic swarm of Aysen Fjord, Chile (2007) associated with two earthquakes (Mw=6.1 and Mw=6.2) within the Liquiñe-Ofqui Fault Zone, *Continental Shelf Research*, 31, 154-161

Legrand D., Calahorrano A., Guillier B., Rivera, L., Ruiz M., Villagómez D., and Yepes H., (2002), Stress tensor analysis of the 1998-99 tectonic swarm of Northern Quito related to the volcanic swarm of Guagua Pichincha volcano, Ecuador, *Tectonophysics*, 344, 15-36

Legrand, D., Villagómez, D., Yepes, H., and Calahorrano, A., (2004), Multifractal dimension and b value analysis of the 1998-1999 Quito swarm related to Guagua Pichincha volcano activity, *Journal of Geophysical Research*, 109 (B0137) doi: 10.1029/2003JB002572.

Matsumura, S., Ohkubo, T., and Imoto, M., (1991), Seismic swarm activity in and around the Izu Peninsula preceding the volcanic eruption of July 13, 1989, *J. Phys. Earth*, 39, 93– 106.

McCaffrey, R., (1992), Oblique plate convergence, slip vectors, and forearc deformation, *Journal of Geophysical Research* 97, 8905–8915.

Mitchell, T.M., and Faulkner, D.R., (2008), Experimental measurements of permeability evolution during triaxial compression of initially intact crystalline rocks and implications for fluid flow in fault zones, *Journal of Geophysical Research*, 113, B11412, doi: 10.1029/2008JB005588

Michael, A. J. (1984), Determination of stress from slip data: Faults and folds, *J Geophys. Res.*, 89, 11,517– 11,526.

Michael, A. J. (1987), Use of focal mechanisms to determine stress: A control study, *J Geophys. Res.*, 92, 357–368.

Mogi, K. (1962), Magnitude-frequency relation for elastic shocks accompanying fractures of various materials and some related problems in earthquakes, *Bull. Earthquake Res. Inst. Univ. Tokyo*, 40, 831–853.

Mogi, K. (1963), Some discussions on aftershocks, foreshocks, and earthquake swarms The fracture of a semi-infinite body caused by an inner stress origin and its relation to the earthquake phenomena, 3, *Bull. Earth quake Res. Inst. Univ. Tokyo*, 41, 615– 658.

Mukhopadhyaya, B., Acharyya, A., Mukhopadhyay, and M., Dasgupta, S., (2010), Relationship between earthquake swarm, rifting history, magmatism and pore pressure diffusion – an example from south Andaman sea, India, *Journal Geological Society of India*, 76, 164-170.

Natawidjaja, D.H., Sieh, K., Ward, S. N., Cheng, H., Edwards, R. L., Galetzka, J., and Suwargadi, B.W., (2004), Paleogeodetic records of seismic and aseismic subduction from central Sumatran microatolls, Indonesia, *J. geophys. Res.*, 109, B04306, doi:10.1029/2003JB002398

Nur A., (1974), Matsushiro, Japan, Earthquake Swarm: Confirmation of the Dilatancy Fluid Diffusion Model. *Geology*, 2, 217-221.

Omori, F., (1895), On the aftershocks of earthquakes. *Coll. Sci. Imper. Univ. Tokyo* 7, 111 –200.

Peltzer, G., Rosen, P., Rogez, F., and Hudnut, K., (1998), Poroelastic rebound along the Landers 1992 earthquake surface rupture, *Journal of Geophysical Research*, 103, 30,131– 30,145, doi: 10.1029/98JB02302.

- Raju, K. A., T., Ramprasad, P. S., Rao, B. R., Rao, and J., Varghese, (2004), New insights into the tectonic evolution of the Andaman Basin, northeast Indian Ocean, *Earth Planet. Sci. Lett.*, 221, 145-162.
- Raju K.A., et al., (2012), Tectonic and volcanic implications of a cratered seamount off Nicobar Island, Andaman Sea, *Journal of Asian Earth Sciences*, 56, 42–53.
- Rittmann A., (1953), Magmatic character and tectonic position of Indonesian volcanoes, *Bull. Volcano.*, 14, 45-58.
- Roman, D., Power, J., Moran, S., Cashman, K., Doukas, M., Neal, C., and Gerlach, T., (2004), Evidence for dike emplacement beneath Iliamna Volcano, Alaska in 1996, *J. Volcanol. Geoth. Res.*, 130, 265–284.
- Rudnicki, J.W., (2001), Coupled deformation–diffusion effects in the mechanics of faulting and failure of geomaterials, *ASME Appl. Mech. Rev.*, 54, 483–502.
- Scholz, C., (1968), The frequency-magnitude relation of microfracturing in rock and its relation to earthquakes, *Bull. Seismol. Soc. Am.*, 58, 399–415.
- Shimazaki, K. (1986), Small and large earthquakes: The effects of the thickness of seismogenic layer and the free surface, in *Earthquake Source Mechanics*, *Geophys. Monogr. Ser.*, 37, 209– 216, AGU, Washington, D. C.
- Simpson, D., Leith, W., and Scholz, C., (1988), Two types of reservoir induced seismicity, *Bull. Seismol. Soc. Am.*, 78, 2025– 2040.
- Smith, W.H.F., and Sandwell, D.T., (1997), Global seafloor topography from satellite altimetry and ship depth soundings, *Science*, 277, 1957–1962.
- Subarya, C. et al., (2006), Plate-boundary deformation associated with the great Sumatra– Andaman earthquake, *Nature*, 440, 46–51, doi:10.101038/nature04522.
- Sykes L., (1970), Earthquake swarms and sea-floor spreading, *J. Geophys. Res.*, 75, 6598-6611.
- Talwani, P., and Acree, S., (1984) Pore pressure diffusion and the mechanism of reservoir induced seismicity, *Pure Appl. Geophys.*, 122, 947–965.
- Talwani, P., Chen, Linyue, Kalpna Gahalaut, (2007), Seismogenic permeability, *J. Geophys. Res.*, 112, B07309 doi:10.1029/2006JB004665.
- Toda, S., Stein, R.S., and Sagiya, T., (2002), Evidence from AD 2000 Izu island earthquake swarm that stressing rate governs seismicity, *Nature*, 419, 58-61
- Walter, T. R., Amelung, F., (2007), Volcanic eruptions following M = 9 megathrust earthquakes: Implications for the Sumatra-Andaman volcanoes, *Geology*, 36, 539-542. doi: 10.1130/G23429A
- Wang, H.F., (2000), *Theory of Linear Poroelasticity*, 287 pp. Princeton Univ. Press, Princeton, N. J
- Warren, N., and Latham, G., (1970), An experimental study of thermally induced microfracturing and its relation to volcanic seismicity, *J. Geophys. Res.*, 75, 4455–4464. Wiemer, S., and Wyss, M.,

(1997), Mapping the frequency-magnitude distribution in asperities: An improved technique to calculate recurrence times?, *J. Geophys. Res.*, 102, 15,115– 15,128.

Wiemer, S., McNutt, S., and Wyss, M., (1998), Temporal and three-dimensional spatial analyses of the frequency-magnitude distribution near Long Valley Caldera, California, *Geophys. J. Int.*, 134, 409– 421.

Wiemer, S., and McNutt, S., (1997), Variations in the frequency-magnitude distribution with depth in two volcanic areas: Mount St. Helens, Washington, and Mt. Spurr, Alaska, *Geophys. Res. Lett.*, 24, 189– 192.

Wright I.C., (1996), Volcaniclastic processes on modern submarine arc stratovolcanoes: sidescan and photographic evidence from the Rumble IV and V volcanoes, southern Kermadec Arc (SW Pacific), *Mar. Geol.*, 136, 21-39.

Wright, T. J., F. Sigmundsson, A. Ayele, M. Belachew, B. Brandsdottir, E. Calais, C. Ebinger, P. Einarsson, I. Hamling, D. Keir, E. Lewi, C. Pagli, R. Pedersen, (2012), Geophysical constraints on the dynamics of spreading centres from rifting episodes on land. *Nature Geoscience*, doi: 10.1038/NGEO1428.

Wyss, M., and Habermann, R., (1988), Precursory seismic quiescence, *Pur Appl. Geophys.*, 126, 319–332.

Wyss, M., Sammis, C. G., Naudeau, R.M., and Wiemer, S., (2004), Fractal dimension and b-value on creeping and locked patches of the San Andreas Fault near Parkfield, California, *Bull. Seism. Soc. Am.*, 94, 410-421, doi:10.1785/0120030054.

Wyss, M., (1973), Towards a physical understanding of the earthquake frequency distribution, *Geophys. J. R. Astron. Soc.*, 31, 341–359.

Figure captions:

Figure.1: Bathymetry (Smith and Sandwell 1997), general tectonics and location of the three swarms of 1983-1984 (by pink ellipse), 1993 (by blue ellipse) and 2005 (by red square) in the back arc region of the Andaman-Sumatra subduction zone. The 2004 Sumatra-Andaman earthquake rupture in the Andaman Nicobar and Sumatra frontal arc (Chlieh et al. 2007) and its epicenter are also shown. Earthquakes before and after the 2004 Sumatra-Andaman earthquake are shown by green and yellow dots respectively. Black arrows show horizontal coseismic offsets from GPS measurements (Gahalaut et al. 2006; Subarya et al. 2006) due to the 2004 Sumatra-Andaman earthquake. Black triangles show active volcanoes in the backarc (Natawidjaja et al. 2004). BV-Barren volcano, IFZ-Investigator Fracture Zones.

Figure.2: Location map of 2005 Andaman Sea swarm along with detailed tectonic features (Curray 2005). The 2004 Sumatra-Andaman earthquake rupture in the Andaman Nicobar and Sumatra frontal arc is shown by red shade. Red hollow triangles are submarine volcanoes (Curray 2005). EMF-Eastern Marginal Fault, SFS-Sumatra Fault System, WAF-West Andaman Fault, SEU-Seulimeum Strand of SFS, WSR-West Sewell Ridge, NSR-North Sumatra Ridge, CN-Car Nicobar Island, T-Teresa Island, K-Katchall Island, LN-Little Nicobar Island, GN- Great Nicobar Island.

Figure.3: Spatio-temporal evolution of the 2005 Andaman Sea swarm since its initiation on 26 January through 31 January 2005. Earthquake epicenters from the EHB catalogue and the available focal mechanisms showing non-double-couple component from the CMT catalogue are shown in the top panels showing. Relative percentage of strike-slip (SS), normal (N) and thrust (T) components in the focal mechanisms in triangular plots is shown in the bottom panels.

Figure.4: Temporal variation of aftershocks of the 2004 Sumatra-Andaman earthquake (right panel) and 2005 Andaman Sea swarm (left panel).

Fig. 5: Bathymetry showing the chain of seamounts in the Nicobar region (Kamesh Raju et al., 2012). Contours in the background are from the world topographic data (Smith and Sandwell, 1997). Black and white pictures in the inset show seafloor images captured by the camera (Kamesh Raju et al., 2012). The depth of the seafloor in the two photographs is indicated.

Figure.6: Static Coulomb stress change (bar) on normal faults (indicated by dashed line in the inset) which lie between WAF and SEU due to the dextral strike slip on the WAF. Temporal change in earthquake focal mechanisms shown by dark green, red, blue, light green and gray colour for the

period 0-24, 24-48, 48-72 and 72-96 and 96-144 hours respectively, from the initiation of the 2005 swarm. The derived principal axes of stress (i.e., s_1 , s_2 and s_3) from the inversion of the fault plane solutions are shown. Stress inversion result of pre-26th December, 2004 Sumatra-Andaman earthquake is also shown.

Figure.7: Gutenberg-Richter law for the period 1973-2010 for total seismicity including the 2005 swarm (curve-A), only for the 2005 swarm (curve-B) and total seismicity excluding 2005 and 1993 and 1983-1984 swarms (curve-C).

Figure.8: Temporal evolution of pore fluid pressure induced change in Coulomb stress (bar) due to coseismic slip on the 2004 Sumatra-Andaman earthquake rupture, in a northeast-southwest vertical cross section in the Nicobar region. Coulomb stress change is resolved on the dextral strike slip WAF. (a) Instantaneous change in Coulomb stress due to the earthquake and (b) its poroelastic relaxation. Note the increase in the change in Coulomb stress from (a) to (b).

Figure.9: Temporal evolution of change in Coulomb stress on the West Andaman Fault (WAF) at 20 km depth (red triangle in Fig.5). Note the effective increase in the Coulomb stress change from about 7 bar (due to the 26th December, 2004 Sumatra-Andaman earthquake) to about 10 bar on the day of initiation of the 2005 swarm).

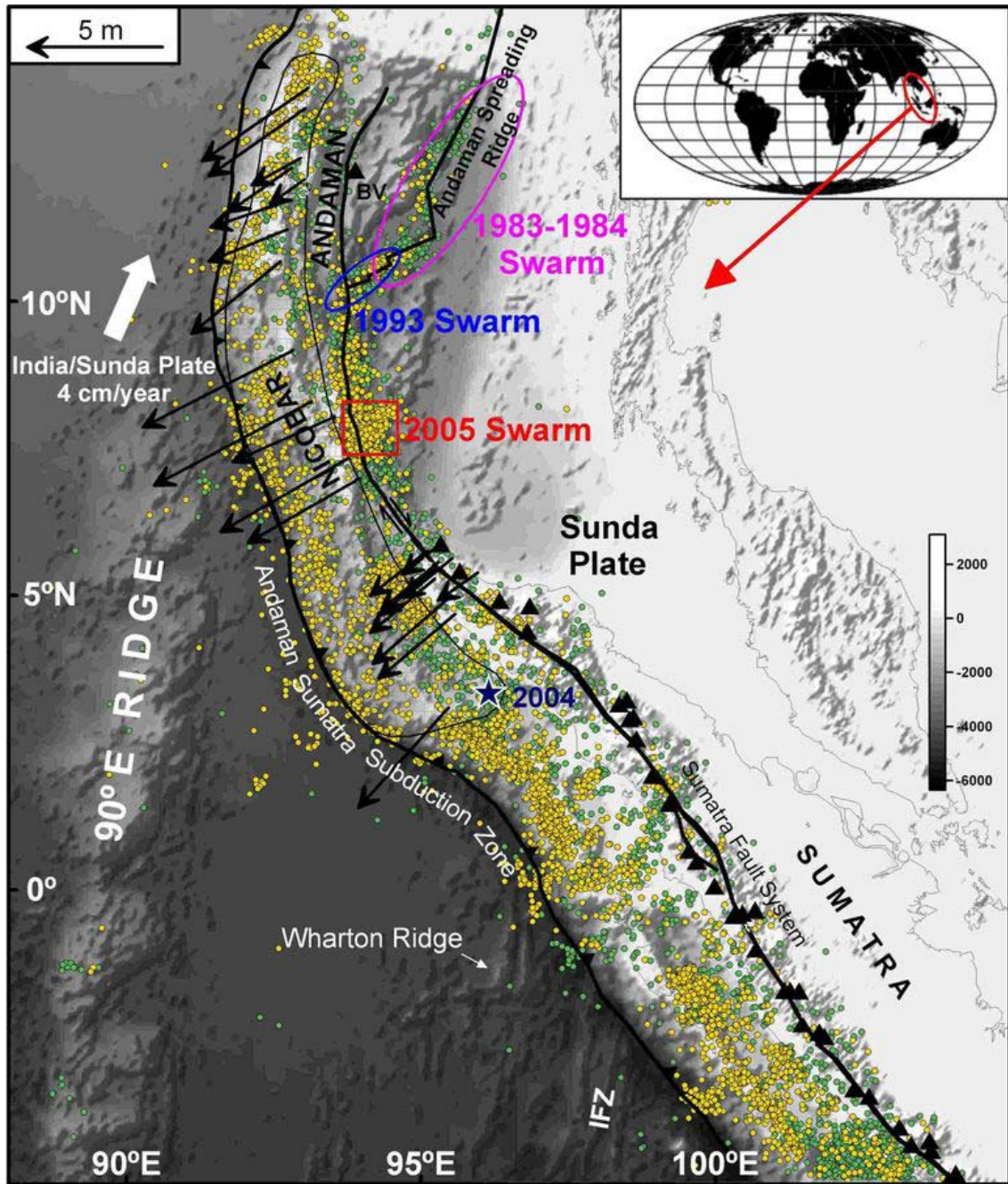


Figure 1

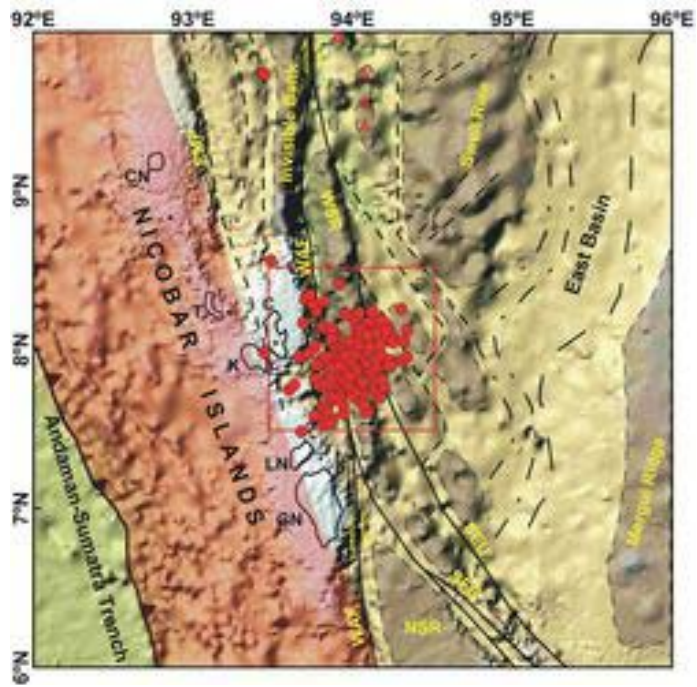


Figure 2

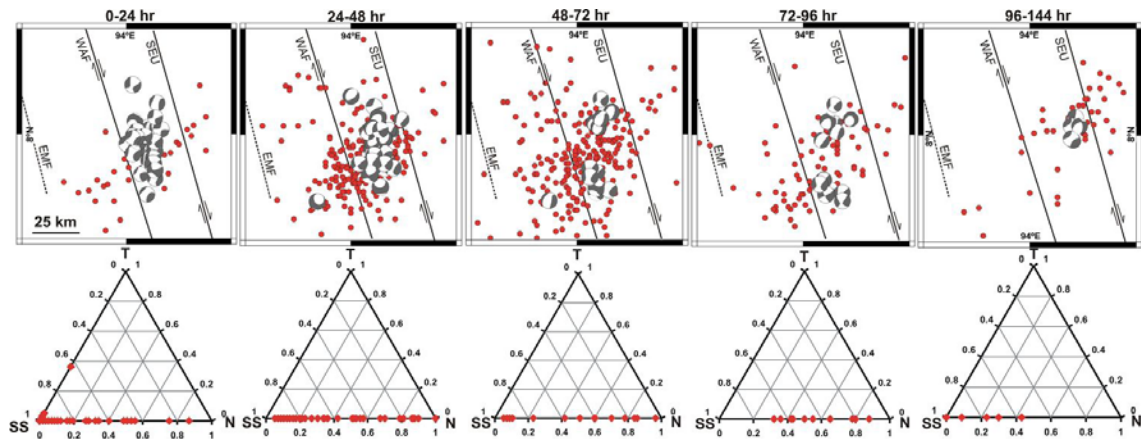


Figure 3

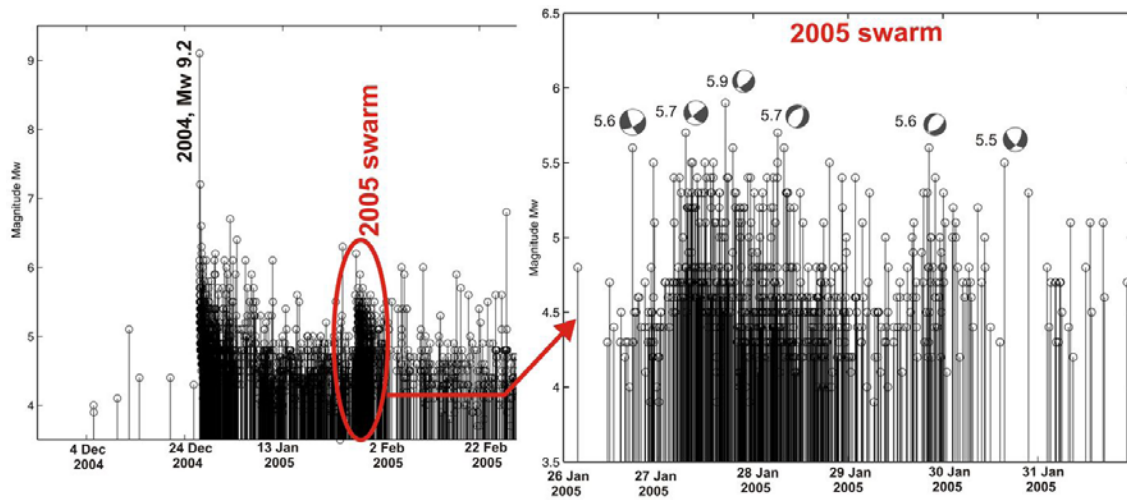


Figure 4

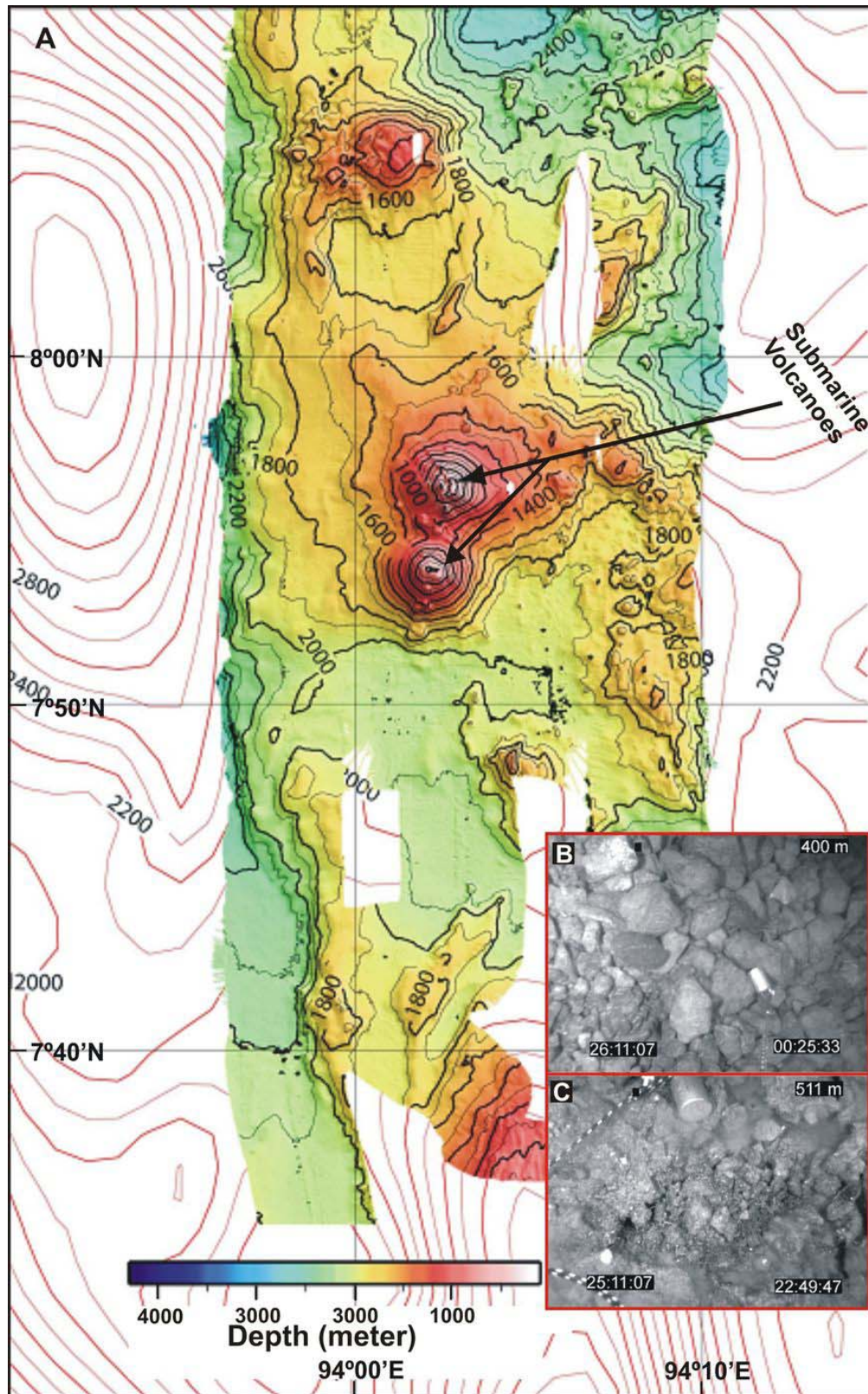


Figure 5

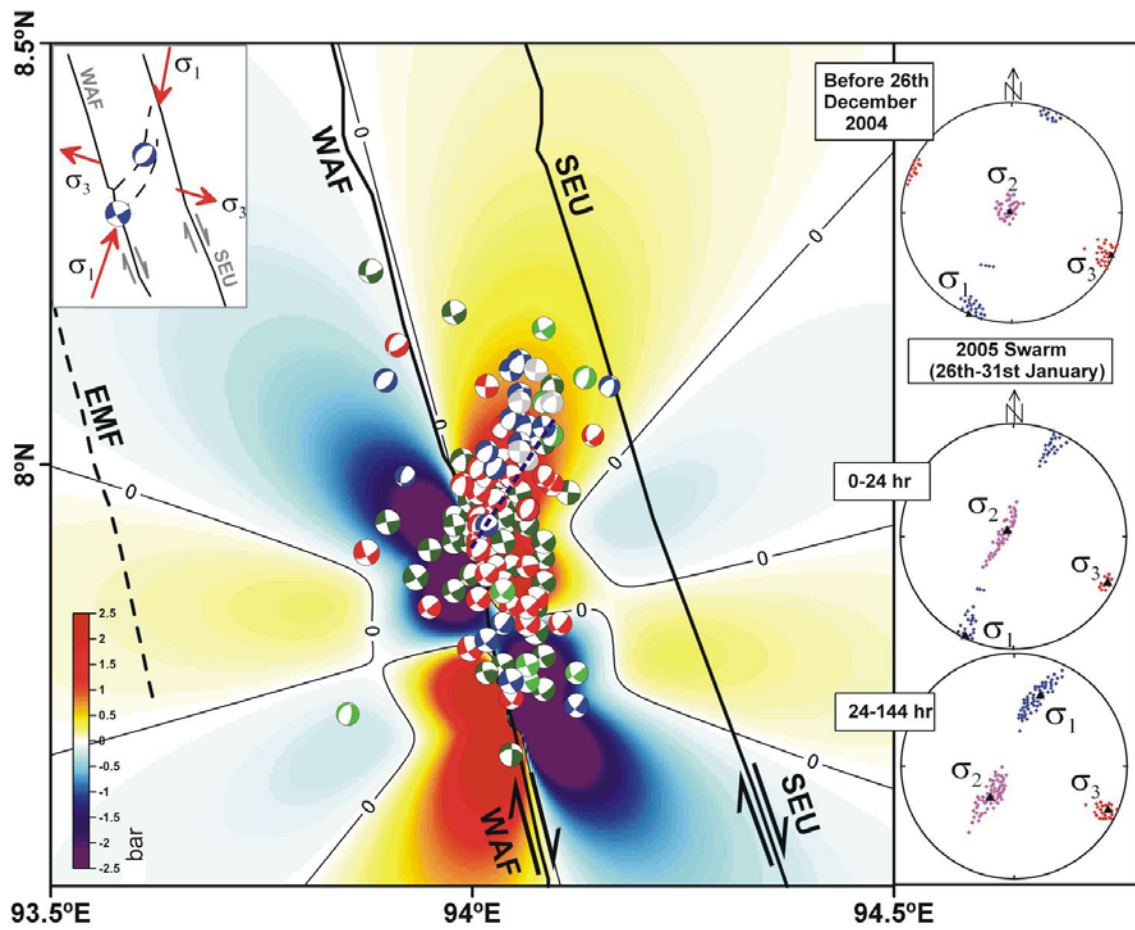


Figure 6

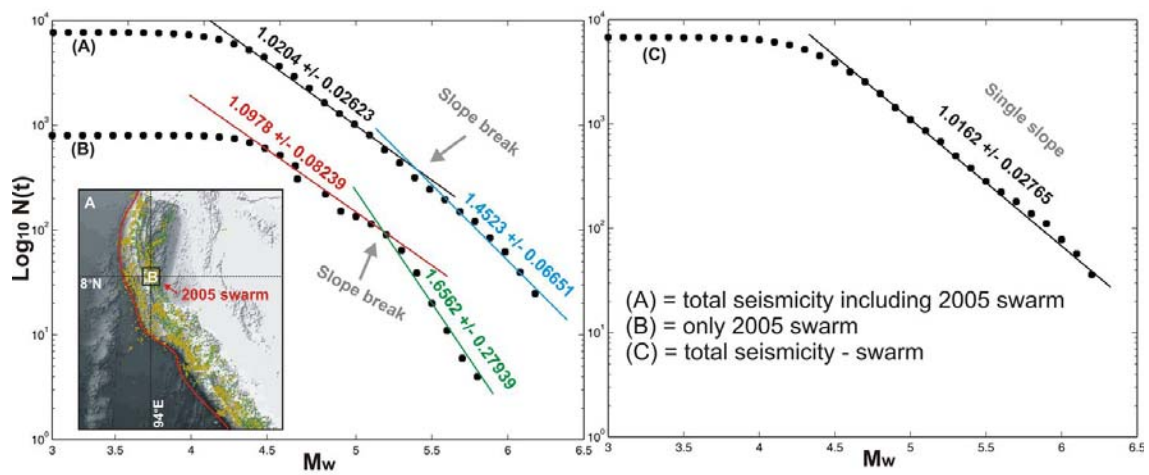


Figure 7

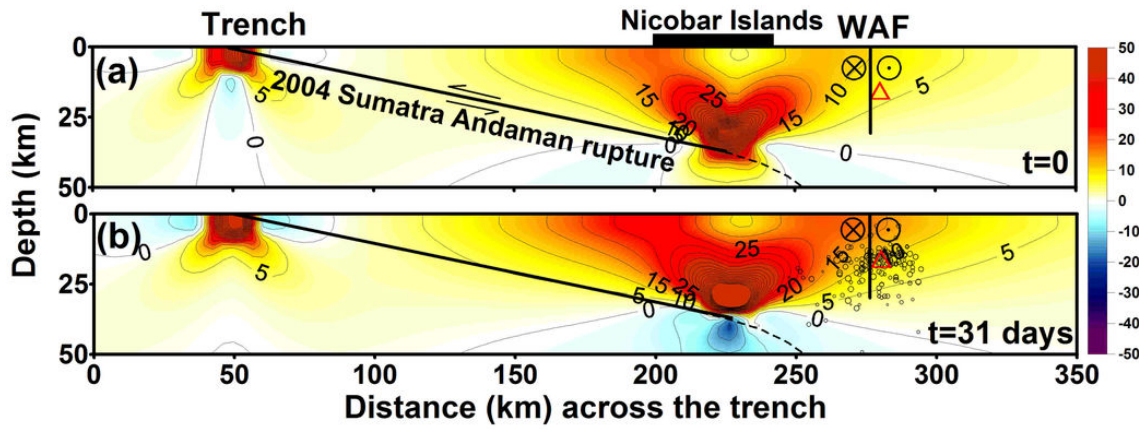


Figure 8

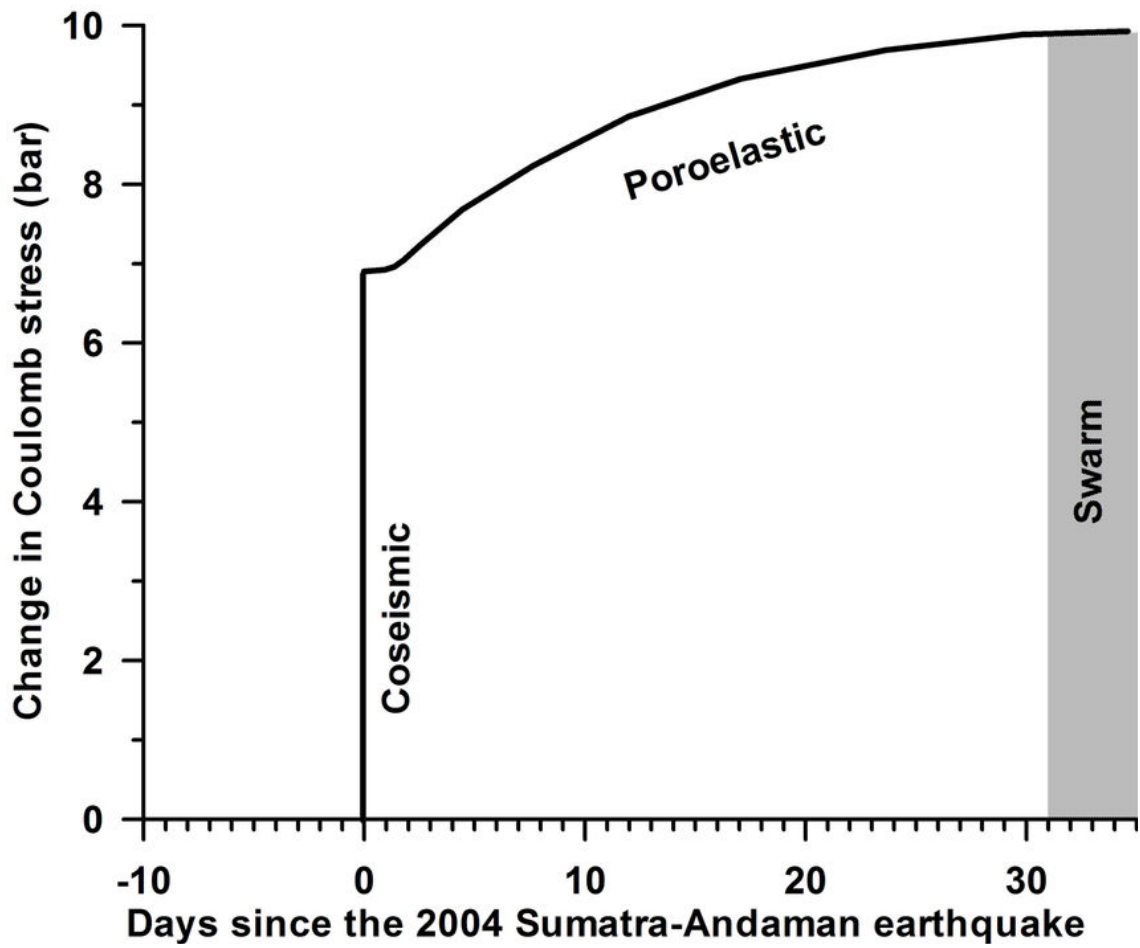


Figure 9